ce/papers Proceedings in civil engineering
eurosteel CRACOW 2026
WILEY

Full paper

Seismic Response Analysis of a 3-story Steel MRF Coupled with Pressurized Sand Dampers

Konstantinos N. Kalfas[1] | Intekhab U.A. Chy[2] | Vasileios C. Kamperidis[3]

Correspondence

Dr. Konstantinos N. Kalfas
Texas State University
Ingram School of Engineering
Civil Engineering Program
San Marcos, TX, 78666
Email: kkalfas@txstate.edu

[1] Texas State University, San Marcos, TX, USA
[2] Rajshahi University of Engineering & Technology, Rajshahi, BD
[3] Neapolis University Pafos, Pafos, CY

Abstract

Seismic resilience is critical in the design of modern structural systems, particularly for steel moment-resisting frames (MRFs). Traditional energy dissipation mechanisms, such as viscous or friction dampers, are effective but often involve high installation and maintenance costs. This study investigates the performance of pressurized sand dampers (PSDs) as an innovative and cost-effective passive control device for mitigating seismic vibrations in steel MRF structures. The proposed system leverages the frictional and dissipative behavior of PSDs. This study presents a numerical analysis using a representative 3-story steel MRF building. The PSD is integrated at selected locations within the frame. Time-history analyses are performed using different earthquake input motions. The study focused on key structural response parameters, including the inter-story drift ratio, the base shear, and the peak floor acceleration comparing the performance of the MRF with and without PSDs. The use of pressurized sand dampers reduces these seismic demands. This research provides insight into the practical implementation of PSDs for seismic control in multi-story steel MRFs, offering a sustainable and adaptable solution for enhancing earthquake resistance.

Keywords

Moment-resisting frames, pressurized sand damper, seismic demand, energy dissipation, seismic resilience

1 Introduction

The concept of response-modification devices is dated back in the 1970s where specially designed devices were developed to offer supplemental energy dissipation and damping to iconic structures like the South Rangitikei Rail Bridge in New Zealand [1-3]. This idea was conceived by Kelly et al. [4] and Skinner et al. [2], who presented it in their seminal studies. Fluid dampers, steel yielding dampers, and buckling-restrained braces (BRBs) comprise the most commonly used response-modification devices that offer supplemental energy dissipation and damping [5-8].

In an effort to develop devices that will not fail when subjected to prolonged displacements [9] and are effective in longer strokes, a device that can accommodate these limitations, in association with offering supplemental damping, has been recently proposed [10-18]. This device is called pressurized sand damper (PSD) and Fig. 1 illustrates a 3D visualization of it, where energy is dissipated from the shearing action of the sand as a sphere, mounted on a piston-rod, plows through the pressurized sand. Previous studies revealed a high performance of the PSDs,

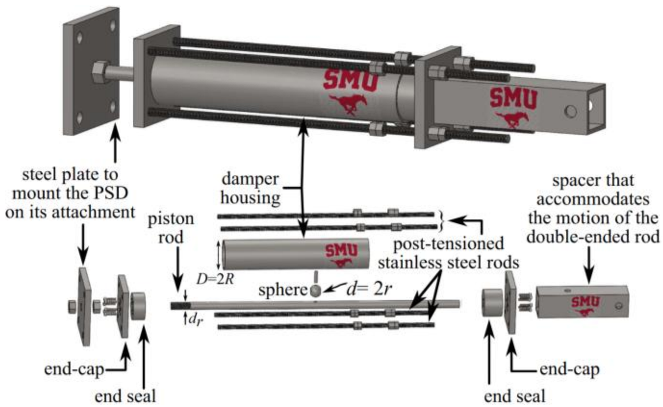

Figure 1 3D visualization of a PSD. Energy is dissipated from the shearing action of the sand as the sphere is plowing through the pressurized sand. The pressure on the sand is exerted with external post-tensioned steel rods, which tensile force is monitored with strain gauges. (Reprinted from [15, 16], © ASCE)

https://doi.org/10.1002/cepa.70771

with no evidence of sand grains escaping from their end seals was observed [11, 13, 14].

In view of the attractive characteristics of PSD that presented in previous studies [10-18], this paper presents a first attempt to assess the seismic response of a 3-story steel moment-resisting frame (MRF) coupled with PSD, representing a typical low-rise buildings in the greater area of Los Angeles, California [19-21].

2 Characterization of the PSD

Past studies on the development of PSD [10, 11, 13, 14] evaluated the effect of geometric properties on the behavior of these devices. The two key design parameters that were evaluated were the clearance ($^{r}/_{R}$), i.e., the distance between the moving sphere and the internal surface of the cylinder, where r is the radius of the sphere and R is the internal radius of the cylinder; and the length of the cylinder ($^{L}/_{R}$), where L is the length of the cylinder.

The findings from these experimental campaigns indicate that the force generated by the PSD at the onset of motion does not depend on the tested clearance ratios. This behavior likely arises from localized failure characteristics of the sand structure near the sphere, as supported by recent numerical results based on discrete deformation analysis [12]. Meanwhile, the experimental findings showed that the force output of the PSD at the onset of motion declines as the cylinder length increases, indicating that the sphere is influenced by the damper finite length even at mid-stroke during motion initiation.

When the measured force–displacement loops across all frequencies and applied pressures are normalized by the strength of the pressurized sand damper, a clear pattern appears, confirming that its behavior is largely rate-independent. The pinching effect observed as the damper stroke grows can be postponed to larger displacements by substituting the sphere on the piston rod with a smaller element, such as a bolt, where only the head and nut extend from the moving rod.

The aforementioned outcomes are supported by the indicative force-displacement loops shown in Fig. 2. Sinusoidal displacement loads, $u(t) = u_0 \sin(2\pi f_0 t)$, were applied, of stroke u_0 and frequency f_0. These loads were applied to different configurations, which were subjected to multiple pressure levels, p. It is noted that the force output as the sphere passes through the origin, where it attains peak velocity during harmonic motion, is nearly independent of velocity. The general form of the hysteretic loops, along with the pinching behavior that appears at larger displacements and higher pressure levels, remains largely unaffected by the local response before yielding.

3 Benchmark MRF building and phenomenological model of the PSD

3.1 Numerical model of the low-rise MRF building

The benchmark structure is the 3-story steel MRF building

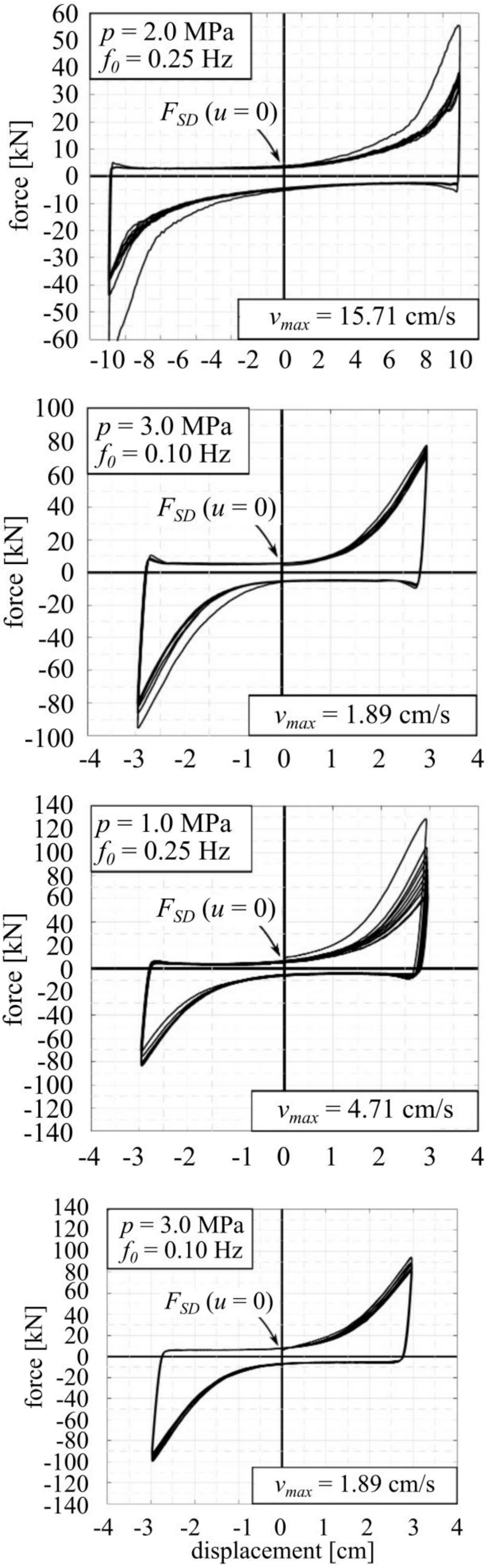

Figure 2 Indicative force-displacement loops from multiple PSD configurations.

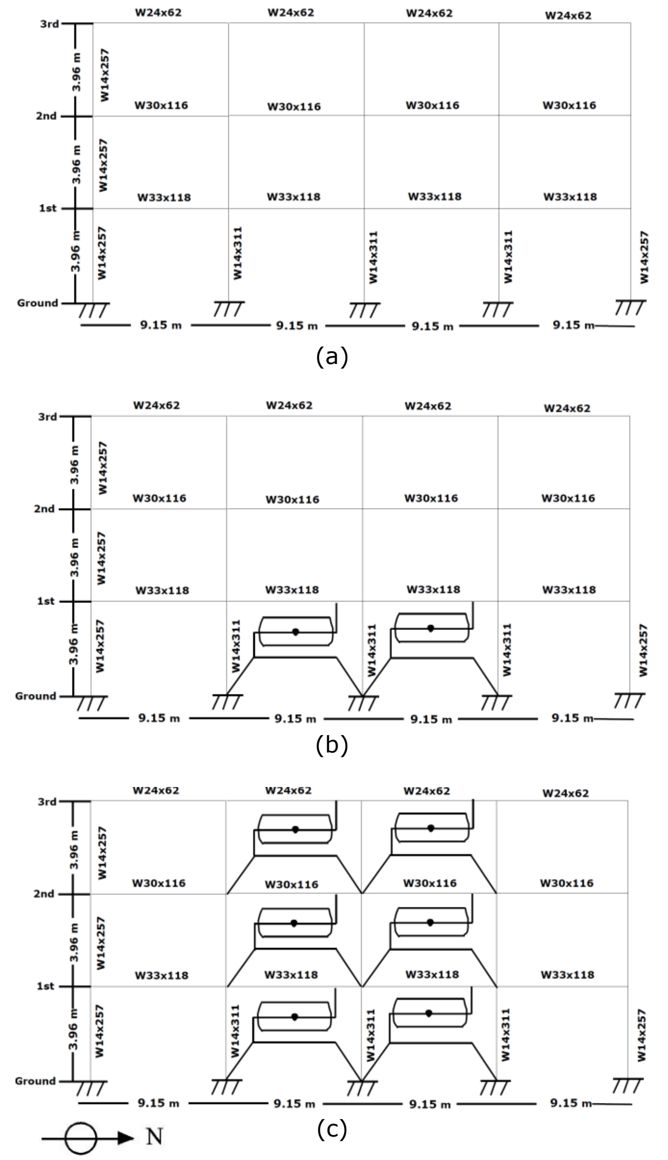

Figure 3 Three-story benchmark steel MRF building of the SAC Phase II Project [22]. (a) Without supplemental PSDs. (b) Coupled with PSDs at the first floor of the two middle bays. (c) Coupled with PSDs in all floors of the two middle bays.

designed for the SAC Phase II Project in the early 2000's [22]. This is a well known structure to the literature [19, 21] that represents a typical low-rise buildings in the greater Los Angeles area, in California.

The configuration of the steel MRF building consists of 3 floors, with 3.96 m height each, resulting in a total building height of 11.88 m, as shown in Fig. 3. The structure has 4 bays, 9.15 m wide, in the north-south (N-S) direction, while there are six bays in the east-west (E-W) direction. The 2D planar analysis in this study is performed with the exterior frame in the N-S direction. There are no column splices, while the column bases are modeled as fixed connections to restrain the structure in the horizontal direction at the foundation level. The same column sizes are used throughout the elevation. The columns are made of wide-flange shapes (W-shape) with a yielding strength of $\sigma_{y,c}$= 345 MPa, which sizes are shown in Fig. 3. The yielding strength of all floor steel section beams is set to be $\sigma_{y,b}$= 248 MPa, and the shape is wide-flange (W-shape) as shown in Fig. 3. All beam-column connections of the frames are rigid (moment resisting connections) except for the further north bay beams, which the beam-column connections are pinned (hinged connections) in order to avoid biaxial bending of the members.

The state-of-the-art open-source software OpenSees [23] is utilized to perform the non-linear response of the 3-story steel, multi-degree-of-freedom (MDOF) MRF building. The OpenSees, nonlinear built-in model Steel01 is used to simulate the W-shape beams and columns properties, which is essentially a bilinear model, at the stress-strain level. The elastic modulus for the building components is set to be E= 210 GPa, with the strain hardening ratio b= 0.03. More details about the modelling of the 3-story MRF building are available in the literature [19-21].

Three different configurations are used in this study. Figure 3 illustrates all three configurations. Figure 3a shows the benchmark structure, where no PSDs are coupled with the building. Figure 3b shows the 3-story MRF coupled with PSDs at the first floor of the two middle bays; while Fig. 3c shows the 3-story MRF coupled with PSDs at all floors of the two middle bays.

3.2 Phenomenological model of the PSD

The phenomenological modelling of the PSD used in this

study is selected based on previous studies [10, 13]. Arguments of dimensional analysis [24-25] and the application of the differential Bouc-Wen model [26-28] are used to approximate the highly non-linear behavior of the PSDs:

$$F_d(\mathrm{t}) = \Pi_{SD}\mathrm{p}R^2 \cdot \left[\eta \mathrm{sgn}\left(\dot{u}(\mathrm{t})\right) + \zeta \mathrm{z}(\mathrm{t})\right] = Q \cdot \left[\eta \mathrm{sgn}\left(\dot{u}(\mathrm{t})\right) + \zeta \mathrm{z}(\mathrm{t})\right] \quad (1)$$

where $z(t)$ is the dimensionless internal time-dependent variable of the Bouc-Wen model that is defined by:

$$\dot{z}(\mathrm{t}) = \frac{1}{u_y} \cdot \left[\dot{u}(\mathrm{t}) - \beta \cdot \dot{u}(\mathrm{t}) \cdot |z|^n - \gamma \cdot |\dot{u}| \cdot \mathrm{z} \cdot |z|^{n-1}\right] \quad (2)$$

The definition of the parameters that appear in Eqs. (1) and (2) and their corresponding values are presented in Table 1. The OpenSees routine followed in this study is similar to past publications [29, 30]

4 Response of the 3-story MRF with PSDs

The three structures under consideration are subjected to two historic earthquake ground motions; the 1995 Kobe, Japan earthquake (Fig. 4d) and the 1987 Superstition Hills, California earthquake (Fig. 5d), with the records obtained from the Kakogawa/90 and the Poe Road/270 stations, respectively [31].

Figures 4 and 5 show the results of this study in terms of the inter-story drift (Figs. 4a and 5a), the normalized shear with respect to the weight of the structure (Figs. 4b and 5b), and the peak floor acceleration (Figs. 4c and 5c); for the cases of the benchmark structure without any PSDs (black, solid lines), with PSDs coupled at the first floor of the two middle bays (black, dense, dashed lines), and with PSDs coupled at all the floors of the two middle bays (black, sparse, dashed lines). The PSD relative strength to the structure mass and the ground acceleration is cons-

Table 1 Parameters of the Bouc-Wen phenomenological model.

Parameters	Definitions	Values
Π_{SD}	Dimensionless parameter	5.12
p (N/mm²)	Exerted pressure on the sand	(-)
R (mm)	Radius of the moving sphere	(-)
η (-)	Dimensionless variables	1
ζ (-)		0.025
$\dot{u}(t)$	Velocity of the piston-rod	(-)
u_y (mm)	Yield displacement	5
β (-)	Hysteresis loop shape control parameters	-3.80
γ (-)		3.43
n (-)	Transition control parameter from the elastic to the yielding regime	1.00
$Q = pR^2$ (N)	Strength of the pressurized sand damper	(-)
m (kg)	Structure mass	(-)
g (m/s²)	Ground acceleration	(-)
Q/mg (-)	PSD strength, relative to the structure mass and the ground acceleration	0.15

sidered Q/mg= 0.15.

By reviewing the inter-story drift ratio (IDR), it is seen in Fig. 4a that the coupling of the 3-story MRF with the PSD reduces it. This reduction ranges from 13.2% on the second floor when the PSDs are coupled at the first floor of the two middle bays (Fig. 3b), to 45.8% on the third floor when the PSDs are coupled to all the floors of the two middle bays (Fig. 3c). When the two cases of the MRF coupled with the PSDs are compared (Figs. 3b and 3c), then the use of PSDs on all floors of the two middle bays results in IDR reduction up to 36.9% on the third floor. Similar patterns are observed in Fig. 5a.

The coupling of the MRF with PSD in different levels resulted in an increase of the base shear when the comparison is between Fig. 3a and Figs. 3b and 3c, up to 18.2% between Figs. 3a and 3b. The different levels of the application of PSDs resulted in similar base shear. Similar trends are observed when the structure is subjected to the stronger 1987 Superstition Hills earthquake, when the two cases with the coupled PSDs are compared. There is a significant increase in the base shear up to 45.2%.

Finally, the peak floor accelerations (PFA) are not consistently reduced from one floor to the other. More specifically, when the structure is subjected to the 1995 Kobe earthquake, there is a reduction of the PFA when the PSDs are coupled to all floors of the two middle bays (Fig. 3c), and there is also a reduction of the PFA when the two cases of the PSDs are compared (Figs. 3b and 3c). Nonetheless, this is not the case when the benchmark structure without any PSDs (Fig. 3a) is compared with the case of coupling

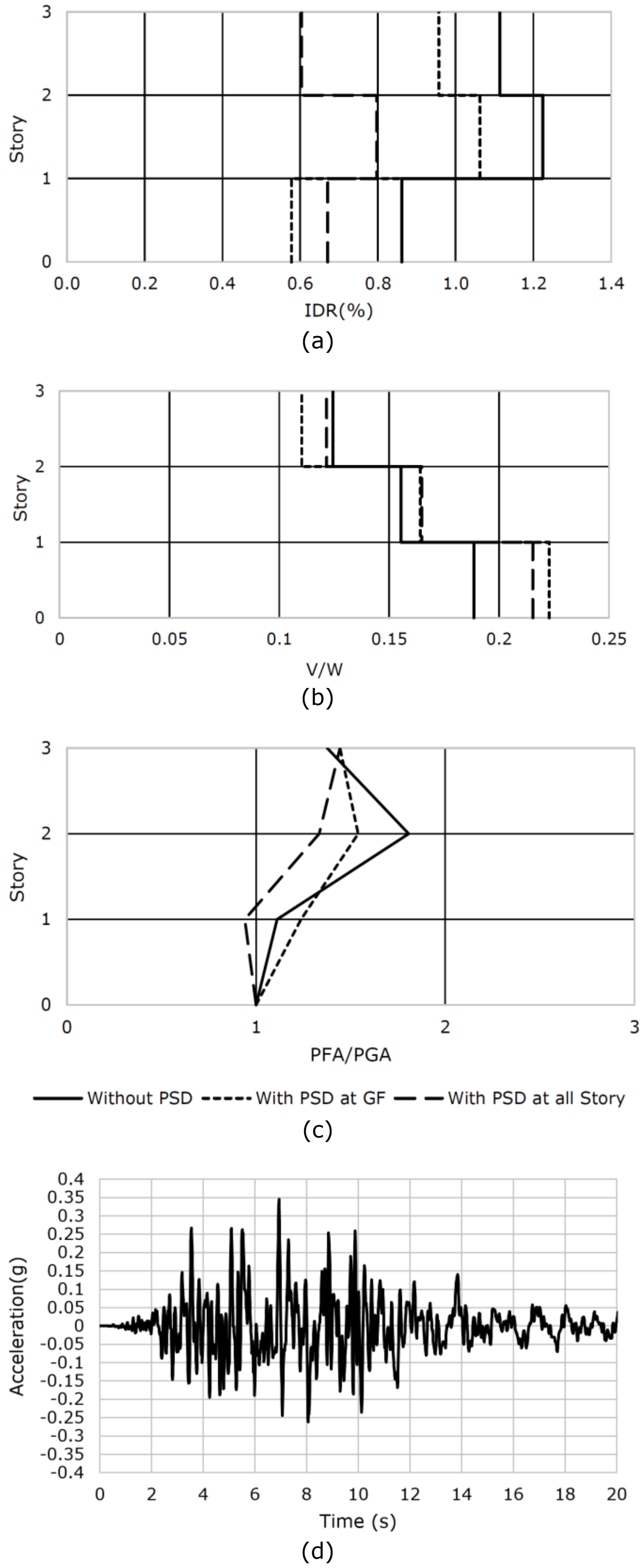

Figure 4 (a) Inter-story drift; (b) normalized shear; and (c) floor acceleration for the three different structures under consideration: w/o PSD (black, solid lines), w/ PSD at first floor in the two middle bays (black, dense, dashed lines), and w/ PSD at all floors in the two middle bays (black, sparse, dashed lines) when subjected to the (d) Kakogawa/90 ground motion recorded during the 1995 Kobe earthquake.

PSDs on the first floor of the two middle bays. On the other hand, when the structure is subjected to the 1987 Superstition Hills earthquake, then there is a PFA reduction either when the benchmark structure without any PSDs (Fig.

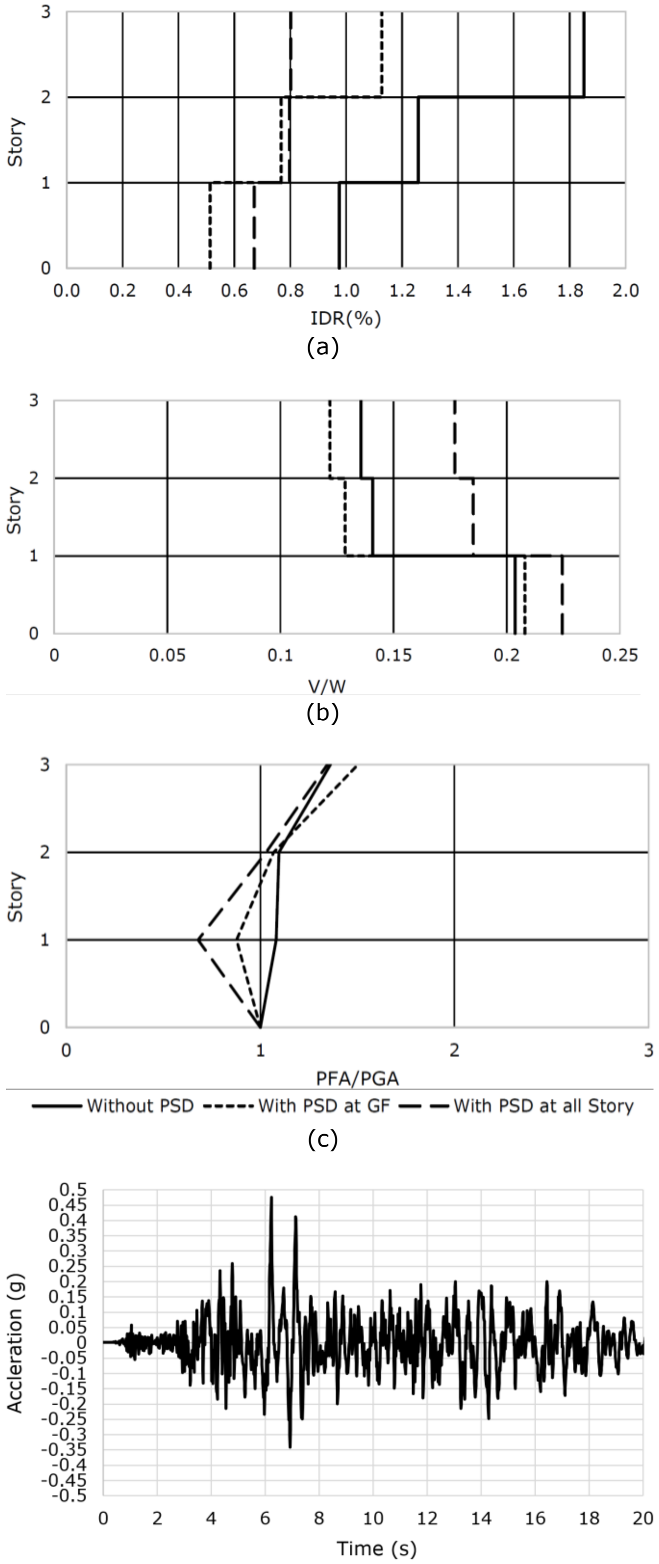

Figure 5 (a) Inter-story drift; (b) normalized shear; and (c) floor acceleration for the three different structures under consideration: w/o PSD (black, solid lines), w/ PSD at first floor in the two middle bays (black, dense, dashed lines), and w/ PSD at all floors in the two middle bays (black, sparse, dashed lines) when subjected to the (d) Poe Road/270 ground motion recorded during 1987 Superstition Hills earthquake.

3a) is compared with the two cases of the structure coupled with the PSDs (Figs. 3b and 3c); or when the two cases of the structure coupled with the PSDs (Figs. 3b and 3c) are compared.

5 Conclusions

This study presented the efficiency of pressurized sand dampers (PSD) as a seismic hazard mitigation technique for low-rise, yielding moment-resisting frame (MRF) structures. The 3-story steel MRF building designed for the SAC Phase II Project was selected as the benchmark case. Two additional cases were studied, one with coupling the PSDs on the first floor of the two middle bays, and one with coupling the PSDs on all floors of the two middle bays. The OpenSees software was used to perform the nonlinear simulations, when the three different structures were subjected to two historic earthquake ground motions.

The results revealed a stable behavior of the system and a more efficient response when the PSDs were coupled on all floors of the two middle bays. The inter-story drift ratios were decreased, as well as the peak floor accelerations, in the cases where the PSDs were coupled to the steel MRF structure. On the contrary, the application of the PSDs invariably decreased the base shear, while in some cases it was increased. These observations are in line with previous studies [29, 30]. This study showed that the PSD can emerge as a resilient and cost-effective solution for the seismic protection of low-rise buildings.

References

[1] Beck, J.L.; Skinner, R.I. (1973) *The seismic response of a reinforced concrete bridge pier designed to step*. Earthq Eng Str Dyn, 2, H. 4, pp. 343–358.

[2] Skinner, R.I.; Kelly, J.M.; Heine, A.J. (1974) *Hysteretic dampers for earthquake-resistant structures*. Earthq Eng Str Dyn, 3, H. 3, pp. 287–296.

[3] Kelly, J.M. (1997) *Earthquake-resistant design with rubber*. London, UK: Springer.

[4] Kelly, J.M.; Skinner, R.I.; Heine, A.J. (1972) *Mechanisms of energy absorption in special devices for use in earthquake resistant structures*. Bull NZ Soc Earthq Eng, 5, H. 3, pp. 63–88.

[5] Black, C.J.; Makris, N.; Aiken, I.D. (2004) *Component testing seismic evaluation and characterization of buckling restrained braces*. J Str Eng, 130, H. 6, pp. 880–894.

[6] Soong, T.T.; Spencer, B.F. (2002) *Supplemental energy dissipation: State-of-the-art and state-of-the-practice*. Eng Str, 24, H. 3, pp. 243–259.

[7] Spencer, B.F.; Nagarajaiah, S. (2003) *State of the art of structural control*. J Str Eng, 129, H. 7, pp. 845–856.

[8] Symans, M.D.; Charney, F.A.; Whittaker, A.S.; Constantinou, M.C.; Kircher, C.A.; Johnson, M.W.; McNamara, R.J. (2008) *Energy dissipation systems for seismic applications: Current practice and recent developments*. J Str Eng, 134, H. 1, pp. 3–21.

[9] Matier, P.; Ross, A. (2013) *Bay bridge shock absorbers spring leak*. San Francisco Chronicle. 19 July

2013.

[10] Makris, N.; Palios, X.; Moghimi, G.; Bousias, S. (2021) *Pressurized sand damper for earthquake and wind engineering: Design, testing, and characterization*. J Eng Mech, 147, H. 4, pp. 04021014.

[11] Kalfas, K.N.; Makris, N. (2022) *Estimation of the design parameters of pressurized sand dampers from experiments*. Proceedings of the ASCE Engineering Mechanics Institute Conference (EMI), Reston, VA: ASCE.

[12] El Shamy, U.; Sabi, E.; Kalfas, K.N.; Makris, N. (2022) *Characterization of energy dissipation during cyclic loading of a sand damper*. Proceedings of the ASCE Engineering Mechanics Institute Conference (EMI), Reston, VA: ASCE.

[13] Kalfas, K.N. (2023) *Component testing and characterization of an innovative pressurized sand damper for the response modification of structures* [Ph.D. Thesis]. Dallas, TX: Southern Methodist University.

[14] Kalfas, K.N.; Makris, N.; El Shamy, U. (2023) *Assessment of the effect of design parameters of pressurized sand dampers from component testing*. J Eng Mech, 149, H. 10, pp. 04023072.

[15] Kalfas, K.N.; Vaiana, N.; Makris, N. (2025) *A rate-independent phenomenological model for the characterization of pressurized sand dampers*. J Eng Mech, 151, H. 4, pp. 04025007.

[16] Kalfas, K.N.; Cao, L.; El Shamy, U.; Ricles, J.M.; Makris, N. (2026) *Behavior of pressurized sand dampers in harsh environments: Extreme temperatures and humidity*. J Str Eng, 152, H. 7, pp. 04026070.

[17] Karimipetanlar, M.; El Shamy, U.; Kalfas, K.N.; Makris, N. (2024) *The influence of particle shape on crushing pattern and energy dissipation within a pressurized sand damper*. Comp Geot, 166, pp. 106020.

[18] Karimipetanlar, M.; El Shamy, U.; Kalfas, K.N.; Makris, N. (2024) *Numerical simulations of particle behavior and crushing within a pressurized sand damper subjected to cyclic loading*. J Eng Mech, 150, H. 1, pp. 04023106.

[19] Gupta, A.; Krawinkler, H. (1999) *Seismic demands for performance evaluation of steel moment resisting frame structures*. Stanford, CA: Stanford University.

[20] Chopra, A.; Goel, R. (2002) *A modal pushover analysis procedure for estimating seismic demands for buildings*. Earthq Eng Str Dyn, 31, H. 3, pp. 561–582.

[21] Ohtori, Y.; Christenson, R.E.; Spencer Jr, B.F.; Dyke, S.J. (2004) *Benchmark control problems for seismically excited nonlinear buildings*. J Eng Mech, 130, H. 4, pp. 366-385.

[22] FEMA. (2000) *SAC venture guidelines development committee*. Accessed: June 1, 2000.

[23] Mazzoni, S.; McKenna, F.; Scott, M.H.; Fenves, G.L. (2006) *Open system for earthquake engineering simulation user command-language manual*. Berkeley, CA: Pacific Earthquake Engineering Research Center, University of California, Berkeley, OpenSees version, 1(3).

[24] Langhaar, H.L. (1951) *Dimensional analysis and theory of models*. New York, NY: Wiley.

[25] Barenblatt, G. I. (1996) *Scaling, self-similarity, and intermediate asymptotics: Dimensional analysis and intermediate asymptotics*. Cambridge, UK: Cambridge University Press.

[26] Bouc, R. (1967) *Forced vibrations of mechanical systems with hysteresis*. Proceedings of the 4th Conference on Nonlinear Oscillations, Prague, CZ: Academia.

[27] Wen, Y.K. (1975) *Approximate method for nonlinear random vibration*. J Eng Mech Div, 101, H. 4, pp. 389–401.

[28] Wen, Y.K. (1976) *Method for random vibration of hysteretic systems*. J Eng Mech Div, 102, H. 2, pp. 249–263.

[29] Moghimi, M.; Makris, N. (2022) *Seismic response of yielding multistory steel buildings equipped with pressurized sand dampers*. J Str Eng, 148, H. 7, pp. 04022071.

[30] Magallón-Cervera, C.; Jaimes, M. (2026) *Seismic control of existing soft-story RC buildings with pressurized sand dampers under narrow-band excitation*. Proceedings of the 13th National Conference on Earthquake Engineering, Oakland, CA: EERI.

[31] PEER Center (2013) *Peer ground motion database*. Berkeley, CA: The Regents of the University of California.